UCRL 3429

UNIVERSITY OF CALIFORNIA

Radiation Laboratory

TWO-WEEK LOAN COPY

This is a Library Circulating Copy which may be borrowed for two weeks. For a personal retention copy, call Tech. Info. Division, Ext. 5545

BERKELEY, CALIFORNIA

DISCLAIMER

This document was prepared as an account of work sponsored by the United States Government. While this document is believed to contain correct information, neither the United States Government nor any agency thereof, nor the Regents of the University of California, nor any of their employees, makes any warranty, express or implied, or assumes any legal responsibility for the accuracy, completeness, or usefulness of any information, apparatus, product, or process disclosed, or represents that its use would not infringe privately owned rights. Reference herein to any specific commercial product, process, or service by its trade name, trademark, manufacturer, or otherwise, does not necessarily constitute or imply its endorsement, recommendation, or favoring by the United States Government or any agency thereof, or the Regents of the University of California. The views and opinions of authors expressed herein do not necessarily state or reflect those of the United States Government or any agency thereof or the Regents of the University of California.

UCRL-3429

UNIVERSITY OF CALIFORNIA

Radiation Laboratory
Berkeley, California

Contract No. W-7405-eng-48

DECAY CHARACTERISTICS AND MASSES OF POSITIVE K MESONS PRODUCED BY THE BEVATRON

Robert W. Birge, Donald H. Perkins, James R. Peterson,
Donald H. Stork, and Marian N. Whitehead

May 31, 1956

Printed for the U. S. Atomic Energy Commission

Contents

Abstract 3

1. Introduction 4

2. General Method

   2.1. Exposure 5

   2.2. Scanning 5

   2.3. Identification of Secondaries

      1. Systematic Following 6

      2. Blob-Counting

         a. Introduction 9

         b. Calibration 9

         c. Blob count on K secondaries 11

         d. Total distribution 12

3. Relative Abundances of the Various Modes of Decay 13

   3.1. τ, τ', and $K_{\mu 3}$ Secondaries

      1. Dark Secondaries 15

      2. Blob-Counted and Followed Secondaries 15

      3. High-Energy $K_{\mu 3}$ Secondaries 15

   3.2. K_{e3} Secondaries 16

   3.3. $K_{\mu 2}$ and $K_{\pi 2}$ Secondaries 16

   3.4. Comparison With Other Data 16

4. Range Measurements on $K_{\mu 2}$ and $K_{\pi 2}$ Secondaries

   4.1. Method 17

   4.2. Mass of the $K_{\mu 2}$ and $K_{\pi 2}$ from Ranges of the Secondaries . . 20

   4.3. Discussion of the Results 21

5. Primary Mass 22

6. Conclusions 23

7. Acknowledgments 25

Appendix: Effect of Scanning Efficiency on Relative Abundances 26

DECAY CHARACTERISTICS AND MASSES OF POSITIVE K MESONS PRODUCED BY THE BEVATRON

Robert W. Birge, Donald H. Perkins, James R. Peterson, Donald H. Stork, and Marian N. Whitehead

Radiation Laboratory
University of California
Berkeley, California

May 31, 1956

Summary. – A large emulsion stack exposed to the positive K beam at the Berkeley 6-Gev Bevatron has been used to measure the mass of the K particles and their abundances. The masses for the decay modes $K_{\mu 2}$, $K_{\pi 2}$ and τ were obtained by measurement of the mean range of the secondaries. In addition, masses for all modes compared to the proton mass were measured by the range-momentum method. The abundances were determined by following and blob-counting secondaries. The data are:

Type	Abundances o/o	Primary Mass (m_e)	Mass from Secondary Range(m_e)
τ	5.56 ± 0.41	966.3 ± 2.1	966.1 ± 0.7
τ'	2.15 ± 0.47	967.7 ± 4	
$K_{\mu 2}$	58.2 ± 3.0	967.2 ± 2.2	965.8 ± 2.4
$K_{\pi 2}$	28.9 ± 2.7	966.7 ± 2.0	962.8 ± 1.8
$K_{\mu 3}$	2.83 ± 0.95	969 ± 5	
K_{e3}	3.23 ± 1.30	967 ± 8	

DECAY CHARACTERISTICS AND MASSES OF POSITIVE K MESONS PRODUCED BY THE BEVATRON

Robert W. Birge, Donald H. Perkins, James R. Peterson, Donald H. Stork, and Marian N. Whitehead

Radiation Laboratory
University of California
Berkeley, California

May 31, 1956

1. - Introduction

In previous communications[1] we have reported on measurements of the masses of positive K mesons by use of the strong-focusing spectrometer of the Berkeley Bevatron. The decay modes of a few of the K_L's were identified by blob-counting the secondaries a few centimeters from the decay point. The masses of these identified K's were then measured by the range-momentum method.

It soon became obvious that any mass difference between the various types of K mesons was so small as to be detectable only by more precise measurements on identified particles. At the same time the small mass differences became of increasing interest as evidence indicated that the $K^+_{\pi 2}$ (θ^+) and the τ meson could not have the same spin and parity configuration[2]. This result indicated that they must either be different particles or be genetically related, as in the cascade scheme[3], wherein either particle might be the decay product of the other. In the latter scheme a range-momentum-type measurement would give the mass of the parent particle only. The half life of the daughter particle is presumed to be so short as to be undetectable.

---

(1) Birge, Peterson, Stork, and Whitehead, Phys. Rev. 100, 430 (1955). Birge, Haddock, Kerth, Peterson, Sandweiss, Stork, and Whitehead, Pisa Conference Report. Supplemento Al Volume III, Serie X Del Nuovo Cimento N. I, 1955.

(2) R. Dalitz, Proceedings of the Fifth Annual Rochester Conference (Interscience Publishers, New York City).

(3) S. B. Treiman and H. W. Wyld, Jr., Phys. Rev. 99, 1039 (1955); T. D. Lee and J. Orear, Phys. Rev. 100, 932 (1955).

From the range measurements of the secondaries from each of the modes $K_{\pi 2}$, $K_{\mu 2}$, τ, we have calculated the Q's of the decays, and therefore the mass of the possible "daughter" particle in the cascade scheme. In following and blob-counting the decay secondaries we have also obtained the relative abundance of the various modes of decay and the decay spectra of the three-body modes involving a single charged secondary, viz. $K_{\mu 3}$, K_{e3}, and τ'. The details of the range-momentum method of measuring the masses of the primary K particles are to be published separately[4]. The analysis of the τ decays obtained in this work has been described previously[5].

The ranges of the secondaries from $K_{\mu 2}$ and $K_{\pi 2}$ particles, the identication of the decay modes, the relative abundances, and the significance of the mass measurements are discussed here. These data are compared with those given by other experimenters.

2. - General Method.

2.1. Exposure. - A nuclear emulsion stack of 95 pellicles, each of thickness 600 microns and area 9 by 17.5 inches, was exposed at the Bevatron to a K-meson beam produced in a copper target at 90° to the primary 6.2-Gev protons. Details of the strong-focusing spectrometer used to form the K beam have been given elsewhere[1,4], but the general features are as follows. A strong-focusing quadrupole magnetic lens forms an image of the target in the stack, at a point about 1 foot behind a bending magnet that serves to separate particles of different momenta. See Fig. 1. The momentum resolution of the system is determined by the magnification of the lens system and dispersion of the bending magnet. In our experiment, this resolution was ± 1.2% in momentum, which, when combined with the K-meson range straggling, resulted in a standard deviation of ± 19 m_e in the determination of the mass of a single K particle by range-momentum measurements. The average proper time of flight was 1.4×10^{-8} second.

2.2 Scanning. - A swath was scanned in each emulsion just beyond the proton range and perpendicular to the beam direction. Each track of appropriate grain density and direction was followed to its end. Observation of

---

(4) James R. Peterson, The Masses of Identified Positive Heavy Mesons (thesis), UCRL-3368, April 1956.

(5) Roy P. Haddock, Nuovo Cimento, in press; also Analysis of One Hundred Bevatron τ^+ Particles, UCRL-3284, Feb. 1956.

one or more tracks of secondary particles at the end point identified the primary as a heavy meson. The distribution in range of such primary particles shows a sharp peak; that of particles with no observed decay is more diffuse but also shows a distinct peak at the same range. The areas under the peaks indicate that about 15% of the secondaries of K particles escaped detection. See Appendix A for discussion of the effect of this loss on relative abundances.

The heavy mesons thus found were classified by the scanners as τ's or K particles with light or dark secondary tracks. The subjective category "dark" includes roughly all secondary tracks of ionization greater than twice the minimum value.

2.3 Identification of Secondaries.

1) Systematic following.

a. The track of each decay secondary was followed if its direction indicated that it had 21 centimeters of emulsion path available. In this way it was possible not only to follow to rest secondaries from the $K_{\mu 2}$ mode, but also to obtain an unbiased sampling of the decay modes. The secondary particles to be distinguished were the π^+ from $K_{\pi 2}$ decay, (R = range ≈ 12 cm); μ^+ from $K_{\mu 2}$, (R ≈ 21 cm); π^+ from alternative decay of the τ, (R_{max} = 3.8 cm); e^+ from K_{e3}; and the μ^+ from $K_{\mu 3}$, (R_{max} ≈ 17 cm, assuming the decay mode $K_{\mu 3} \rightarrow \mu^+ + \pi^0 + \nu$).

Of course not all tracks could be followed to the ends of their ranges, because some of the π mesons interacted in flight, some tracks of all varieties were lost out of the stack by accumulated Coulomb scattering, and a few very flat tracks were lost between pellicles. All secondary tracks not stopped were blob-counted as far along the track as possible, and are listed in Table I.

For tracks not stopped, the separation of the remaining modes was based on the blob count and on the following arguments. The relative yield of K's decaying into the three-body modes such as the $K_{\mu 3}$ and K_{e3} is about 6%,* and in addition only a fraction of their secondary energies are high enough to be confused in this analysis with a $K_{\mu 2}$ or $K_{\pi 2}$ secondary. Hence, tracks satisfying the ionization criterion for $K_{\pi 2}$ secondaries when leaving the stack have been listed as π's even though they might have been μ's from $K_{\mu 3}$ decay.

* See Section III.

Table I – Path length of nonstopped particles obtained from systematic following of secondaries.

Events identified $K_{\mu 2}$	Secondary Range (cm)	Type of ending	Events identified $K_{\pi 2}$	Secondary Range (cm)	Type of ending
1	6	+	1	1	*
2	6	+	2	2	*
3	6	0	3	3.5	*
4	7	0	4	4	*
5	7	0	5	5	§
6	7	+	6	6	*
7	9	0	7	6.5	+
8	9	0	8	7	0
9	9	+	9	7	*
10	9	+	10	9	*
11	10	0	11	11.5	0
12	10	0			
13	10	§			
14	11	0			
15	11	§			
16	11	+			
17	11	+			
18	11	0			
19	12	0			
20	12	§			
21	12	0			
22	13	+			
23	13	+			
24	14	0			
25	14	0			
26	15	0			
27	15	0			
28	16	0			
29	17	+			
30	17	0			
31	17	0			
32	17	0			
33	17	0			
34	18	0			
35	19	0			
36	19	0			
37	19	0			
38	20	0			
39	20	0			
40	21	0			

* = star in flight
0 = out of stack
\+ = lost
§ = stopped following

Only four secondaries were classified as $K_{\pi 2}$ in this manner, and therefore it is unlikely that one could have been a μ. Secondaries making a star in flight are also listed as π's from $K_{\pi 2}$ decay, having been separated from τ' secondaries on the basis of blob count.

The forty tracks leaving the stack at nearly minimum ionization have been called μ's from $K_{\mu 2}$. All had path lengths in the stack greater than 6 cm. Of these, 25 had path lengths less than 14 cm. We estimate that about 1% of these could be μ's from $K_{\mu 3}$, and the only other alternative, the e^+, should have been easily recognized after 6 cm by its characteristic energy loss and associated scattering. Considerable attention was given to the possibility of the incorrect identification of those secondaries that left the stack at 6 to 9 cm, which could have been high-energy electrons rather than μ mesons from $K_{\mu 2}$ decay. The data indicate that the possibility of such a misinterpretation is remote.

The number of events in each category obtained from the systematic following of secondaries as described above is shown in Table II.

Table II. – Numbers of particles identified by systematic following of secondaries.

Primary	Secondaries			
	Ending in stack	stars in flight	Not stopped	Total
$K_{\mu 2}$	20	0	40	60
$K_{\pi 2}$	20	7	4	31
$K_{\mu 3}$	2	0	0	2
K_{e3}	2	0	0	2
τ'	2	0	0	2
				97

Three additional $K_{\pi 2}$ secondaries were stopped out of a group of 75 secondaries described in Section III.A.

2) Blob-Counting of Secondaries.

a. Introduction.

The proportion of K_L particles that could be identified by following the secondary particles was only of the order of 2.5%, and it was felt desirable to attempt the identification of further K particles by other methods. Information regarding the velocity of emission of the secondary particles can be obtained by measurement of the track density close to the point of decay. It is known, from the foregoing results, that of those secondaries of $\beta > 0.7$, corresponding to values of the specific ionization below 1.3 times the minimum value, the great majority (~87%) result from the $K_{\mu 2}$ and $K_{\pi 2}$ modes of decay. In both cases, the secondary is monoenergetic, the ratio of the values of specific ionization being $I_{\pi 2}/I_{\mu 2} \approx 1.15$. If the statistical fluctuations associated with the measurement of track density can be made sufficiently small, the secondaries may be resolved into one or other category with fairly high efficiency.

In order to specify the ionization of a secondary particle, it was decided to measure the blob density in the track. The blob density is the number, per unit track length, of clearly resolved grains or clusters of grains, and is also therefore the total number of visible gaps per unit length. Blob counting is particularly suited to tracks produced by particles of ionization close to the minimum value, and has the advantages of rapidity of measurement and minimum subjective errors.

b. Calibration.

In order that the measured blob density b may be interpreted in terms of the ionization of the particle, it is necessary to refer it to that of the track of a particle of known ionization, occurring in the same region of the emulsion. The momentum of the particles entering the stack was ≈ 360 Mev/c. Pions of this momentum have a range of 35 cm of emulsion. In order to calibrate the emulsions, it was convenient to make blob counts on the tracks of these pions at a depth of 7 cm into the stack, i.e., at about the same depth as the end points of the K-particle tracks. At this depth, the pions, with a residual range of the order of 28 cm, have practically the same velocity--and hence tracks of the same blob density--as the $K_{\mu 2}$ secondaries. For convenience, the mean blob density in the tracks of these pions or of the $K_{\mu 2}$ secondaries will be called the standard blob density and denoted by b_0.

The emulsion stack was developed in several batches, each batch containing 12 consecutive emulsion sheets. All emulsions in a given batch were processed simultaneously under identical conditions. Counts were made on pion tracks in each emulsion of the development batches used for the blob-count measurements. The blob densities at different emulsion depths were recorded, and hence the variation of development with depth was obtained. Within the statistical errors of the observations, this depth dependence appeared to be much the same in the different emulsions, and the depth variation assumed in the subsequent analysis was that obtained by combining the data from all the emulsions calibrated. It was found that the blob density varied through the emulsion depth by some ±6% about the mean value. Relative to this mean value, that at any particular depth was determined within a statistical error of ±1%.

The fluctuations of development between individual emulsions of a given batch were next investigated. These fluctuations comprise not only variations in sensitivity and degree of development from one emulsion to another, but also variations over the surface area of a particular emulsion. In each emulsion, b_0 was found within a statistical error of 2.5%, and internal fluctuations of b_0 between emulsions in a particular batch were consistent with this value. If real variations within such a batch existed, they were undetectable and cannot have been greater than 1%.

In the absence of such fluctuations, the value of b_0 for a particular emulsion was assumed to be equal to the mean value of b_0 for the batch. As the analysis proceeded, more $K_{\mu 2}$ secondaries were identified by tracing them to rest, and counts were made on the tracks of these particles in order to check the values of b_0 obtained from the pion tracks. The secondaries were traced from emulsion to emulsion in a batch, for distances up to ~ 3 cm from the origin, small corrections being applied to take account of the effect of slowing down. In Table III, the values of b_0 are given for four development batches in which both types of calibration were employed; the data from the pions and from $K_{\mu 2}$ secondaries are displayed separately. The two sets of data are in fair agreement, and the mean, shown in the last column, is the final value of b_0 adopted for a particular batch. The statistical error on this value of b_0 is of the order of 1%, and the variations of b_0 between different development batches greatly exceed this figure. This can presumably be accounted for by the fact that the various batches

were processed at different times and in some cases were made up from different manufacturers' batches of emulsion. The processing procedure was as nearly as possible the same for the different development batches.

Table III. – Values of b_0 for four development batches.

Batch No.	Emulsion No.	Calibration pions		$K_{\mu 2}$ secondaries		Mean b_0
		No. of blobs	b_0	No. of blobs	b_0	
2	15 - 27	13,308	151.5 ± 1.3	10,711	151.3 ± 1.5	151.4
3	28 - 36	6,453	161.3 ± 2	8,023	154.4 ± 2	157.5
5	50 - 60	10,686	158.0 ± 1.5	5,722	161.3 ± 2	159.6
6	61 - 66	6,496	174 ± 2	5,297	178 ± 2.5	176.0

c. Blob counts of K secondaries.

During the scanning of the emulsion stack, the approximate angles of dip of the K secondaries were recorded. From the events observed in the development batches previously calibrated, those K secondaries were selected which had recorded dip angles less than 22°, corresponding to projected track lengths $l_p > 1.5$ mm per emulsion. Blob counts were made on these, totaling 183 tracks. It is convenient to group the tracks into two categories as follows.

Class A consists of secondaries of $l_p < 5$ mm. The track was followed from the point of decay, and blob-counted along its entire length in the next emulsion. If necessary further counts were made in succeeding emulsions, until at least 600 blobs were obtained. For the track densities and lengths in this category, counts had in practice to be made in one, two, or three emulsions. Since the tracks are approximately rectilinear, the blob densities found in this way are practically independent of the variation of development with depth. The blob density was calculated from the total number of blobs and true track length calculated from l_p and assuming an emulsion thickness of 600μ. The average number of blobs counted on Class A tracks was 855.

Class B contains the remaining secondaries, of $\ell_p > 5$ mm. It will be clear that, for very flat tracks, the total angle of multiple scattering may become comparable with the initial angle of dip. Flat tracks are therefore not even approximately rectilinear, and the mean blob density taken over the entire length is dependent on the depth variation. The procedure adopted for Class B tracks was to count at least 700 blobs, either in the emulsion containing the point of decay, if the track length in this emulsion was sufficient, or in the next emulsion if it was not. Counting near the top surfaces of the emulsions was avoided, since there the depth variation was most rapid. The required number of blobs was obtained in practice over a length of about 5 mm, and in this interval, as for Class A tracks, the path of the secondary was assumed to be rectilinear. The depths in the emulsion of the end points of the count were determined, and from the measured blob density and the standard value b_0 appropriate to the mean track depth and development batch, the ratio $b^* = b/b_0$ was calculated. The average number of blobs on Class B tracks was 750.

d. Total distribution.

The distribution in the values of b^* so obtained is shown in Fig. 2. In addition, the secondaries were divided into three groups: Class A secondaries of length $1.5 < \ell_p < 3$ mm (dip angle $22^\circ > \theta > 11^\circ$); the remaining Class A secondaries of $3 < \ell_p < 5$ mm (dip angle $11^\circ > \theta > 6^\circ$); and Class B secondaries of $\ell_p > 5$ mm and $\theta < 6^\circ$. The mean values of b^* for the three histograms were $1.03 \pm .01$; $1.05 \pm .01$; and $1.04 \pm .01$ respectively. Thus, within the limits of dip angle considered (0° to 22°), systematic errors in b^* arising from possible change in the blob-count convention with angle of dip appear to be of the order of 1% or less. This result is in strong contrast with that of Barkas, Heckman, and Smith[6], who obtain a 10% increase in blob density as θ increases from 0° to 16°. A comparison of the histograms for Class A tracks and for Class B tracks also indicates that systematic errors in the assumed variation of blob density with depth in the emulsion are equally negligible.

Included in the histogram shown in Fig. 2, and shown shaded, are the values of b^* for a few secondaries that were identified independently by following them to rest. In order to obtain results of greater statistical weight

(6) Barkas, Heckman, and Smith, Nuovo Cimento Serie X, 3, 85 (1955).

some of the $K_{\mu 2}$ secondaries so identified were also blob-counted in several emulsions (the $K_{\mu 2}$ calibration tracks described above), and the resulting distribution is shown separately in Fig. 3. The average number of blobs counted for each point in Fig. 2 was 815; in Fig. 3, 825.

The standard deviation of the histogram in Fig. 3 is ≈ 4%. The curves in Fig. 2 show the expected Gaussian distributions in b^* for 180 tracks, for an assumed standard deviation of 4%, a mean value of b^* for the tracks of $K_{\pi 2}$ secondaries of 1.145, and a ratio of the frequencies of the two modes of decay $N_{K_{\mu 2}}/N_{K_{\pi 2}}$ of 2.0. For this choice of parameters, the observed and expected distributions are in good agreement. It will be seen that the expected number of μ secondaries of $b^* > 1.07$ is about equal to the expected number of π secondaries of $b^* < 1.07$. The observed ratio of numbers of events of b^* less than and greater than 1.07, excluding identified $K_{\mu 3}$'s, is $118/62 = 1.90 \pm 0.30$.

3. – Relative Abundances of the Various Modes of Decay

In computing the relative abundances of the various modes of decay, it must be borne in mind that the samples used change with the manner in which the secondaries are identified. For example, a blob count at the decay point does not distinguish between the $K_{\mu 2}$ and the K_{e3} modes, or between a $K_{\pi 2}$ secondary and a μ secondary of energy ~ 80 Mev from the $K_{\mu 3}$ mode.

The data from which the final abundances are derived are displayed in Table IV. For each mode of decay, the actual number of events found, and the correct sample size, are given. The latter is derived in a manner discussed below.

The total percentages of the τ' and $K_{\mu 3}$ types have been obtained by adding the percentage found by the scanners to the percentage found in systematically following or blob-counting secondaries. The procedure thus utilizes all available data and gives a result independent of the variation of efficiency of dark-track recognition with secondary ionization. This combining procedure requires, however, that the efficiency of dark-secondary recognition and the efficiency for finding any secondary both have the same distribution in dip angle (since only flat secondaries were systematically studied). The dip angles of all dark secondaries were measured and compared to the dip-angle distribution of 100 other secondaries randomly selected. The distributions were found to be the same and corresponded to spatial isotropy.

Table IV. – Corrected abundances

K-Particle Type	Secondary energy interval	Stack 20			Stack 16A			Combined data		
		No. Found	Sample	Percent	No. Found	Sample	Percent	No. Found	Sample	Percent
τ		112	2272	4.93 ± 0.46	59	803	7.35 ± 0.96	171	3075	5.56 ± 0.41
τ'	D.S.*	32	2272	1.41	16	803	1.99	48	3075	1.56
	Systematic following and blob count	2	320	0.63	0	20	0	2	340	0.59
	All			2.04 ± 0.51			1.99 ± 0.50			2.15 ± 0.47
$K_{\mu 3}$	D.S.*	7	2272	0.31	2	803	0.25	9	3075	0.29
	0-60	4	320	1.25	1	20	5.00	5	340	1.47
	60-80	2	186	1.07				2	186	1.07
	80-90	0	124	0				0	124	0
	90-110	0	91	0				0	91	0
	110-135	0	71	0				0	71	0
	All			2.63 ± 0.97						2.83 ± 0.99
K_{e3}	Systematic following	6	186	3.23 ± 1.30				6	186	3.23 ± 1.30
$K_{\mu 2}$		See Text								58.5 ± 3.0
$K_{\pi 2}$										27.7 ± 2.7

* D.S. represents dark secondaries recognized by scanners.

As described in Section 2.2, the over-all efficiency for detecting a K secondary during scanning is 85%. It will be assumed that the efficiency for detecting secondaries of ionization greater than 1.3 x minimum (though not necessarily recognizing them as such) is 100%.

3.1 τ, τ', and $K_{\mu 3}$ Secondaries.

1) Dark Secondaries. – Those τ, τ', and $K_{\mu 3}$ secondaries recognized by the scanners as being darkly ionizing, were found among a total of 1930 K-meson endings. Correcting for the over-all scanning efficiency, we have a total of 2272 K mesons. In this sample, there were found 112 examples of τ, 37 of τ', and 7 of $K_{\mu 3}$.

2) Secondaries Blob-Counted and Followed. – Ninety-seven secondaries were systematically followed and 183 blob-counted as described in Sections 2.3-1 and 2.3-2. In addition, a further 75 secondaries were followed for a distance of between 5 and 8 cm (a mean of 6.5 cm), in order to find additional examples of $K_{\mu 3}$ and K_{e3}. Of the 183 secondaries blob-counted, 107 were duplicated in the systematic following. The cases of τ' and low-energy $K_{\mu 3}$ (0 to 60 Mev) systematically found came therefore from a sample of 248 K secondaries. The samples studied excluded cases of τ and τ', and of $K_{\mu 3}$ found by dark-secondary recognition, which amount to 7.4% of all K's, and therefore represented 92.6% of an unselected sample of K mesons. After correction for scanning efficiency and for τ's and initially recognized dark secondaries, the sample number becomes 320. This correction has been made in Table IV.

3) High-Energy $K_{\mu 3}$ Secondaries. – Those $K_{\mu 3}$'s of secondary energy exceeding 60 Mev (ionization below 1.3 times minimum) could be found only by systematic following. For example, 172 secondaries were followed a distance such that a 70-Mev muon would have been identified. After correction for K's with recognized dark secondaries, the sample number becomes 186. The $K_{\mu 3}$ data have been grouped in Table IV for several secondary energy intervals. The number of K mesons in the samples diminishes at higher muon energies, as the number of secondaries followed out to sufficiently great distances to ensure identification becomes progressively smaller.

3.2 K_{e3} Secondaries. – K_{e3} secondaries were found only by following 172 K-meson secondaries, or in a sample of 186 K mesons of all types. The shortest distance followed, for which the secondary remained near minimum ionization, was 5 cm. Ninety-three percent of the secondaries were followed 6 cm or otherwise identified, and 76% of the secondaries were followed at least 9 cm or otherwise identified (i.e., observation of star in flight, or ionization above plateau). Such K_{e3} secondaries as were found were readily identified by observing the increase in multiple scattering of their tracks, which typifies large energy losses. At 6 cm, 90% of the electrons will lose more than 3/4 of their energy, while at 9 cm essentially all lose 3/4 of their energy. Thus, we estimate that our over-all efficiency for discriminating between 250-Mev electron secondaries and $K_{\mu 2}$ secondaries was better than 96%. The six electron secondaries found in the above samples had $p\beta = 73$, 75, 80, 100, 183, and 200 Mev/c.

3.3 $K_{\mu 2}$ and $K_{\pi 2}$ Secondaries. – One hundred forty-nine $K_{\mu 2}$ and 77 $K_{\pi 2}$ were found by the methods described in Sections 2.3-1 and 2.3-2. From their ratio, corrected for scanning efficiency (Appendix A), and the total percentage of $K_{\mu 2}$ and $K_{\pi 2}$, the percentage of each was determined.

Additional data obtained from a smaller stack[1] (16A) are shown in Table IV. The data from both stacks has been combined in the last column.

3.4 Comparison With Other Data. – In Table V our results are compared with nuclear-emulsion-stack results from other laboratories[7], [8], [9], [10], [11], [12]. The abundances for the τ' and the $K_{\mu 3}$ in the first three columns have been derived from the published data by means of the methods described in Sections 3.1 and 3.2. The data of columns 2 and 3 have been corrected for scanning

(7) G-Stack Collaboration, Nuovo Cimento 2, 1063 (1955).

(8) Ritson, Pevsner, Fung, Widgoff, Zorn, Goldhaber, and Goldhaber, Phys. Rev. 101, 1085 (1956).

(9) Crussard, Fouche, Hennessy, Kayas, Leprince-Ringuet, Morellet, and Renard, Nuovo Cimento 3, 731 (1956).

(10) Smith, Heckman, and Barkas, Composition of a Secondary-Particle Beam from the Bevatron, UCRL-3289, March 1956.

(11) Hoang, Kaplon, and Yekutieli, Phys. Rev. 102, 1185 (1956).

(12) O'Ceallaigh, Alexander, and Johnson, Proceedings of Sixth Annual Rochester Conference on High-Energy Physics, 1956.

Table V. – Comparison of abundances from different laboratories.

	G.S.[7]	E.P.[8]	MIT[9]	S.H.B.[10]	Rochester[11]	Dublin[12]	Our data
τ	(5.6)	(5.6)	(5.6)	7.8 ± 1.4	5.2 ± 1.6	6.5 ± 0.6	5.56 ± 0.41
τ'	1.1 ± 0.6	0.8 ± 0.4	1.6 ± 0.8	1.9 ± 0.8	3.5 ± 1.4	3.9 ± 1.6	2.15 ± 0.47
$K_{\mu 2}$	63 ± 8	57 ± 6	60 ± 10	65.2 ± 10.3	59 ± 8	51.0 ± 5.7	58.5 ± 3.0
$K_{\pi 2}$	19 ± 5	25 ± 5	20 ± 10	21.4 ± 5.6	21 ± 6	27.5 ± 4.2	27.7 ± 2.7
$K_{\mu 3}$	2.5 ± 1.2	3.8 ± 2.3	1.3 ± 0.7	1.1 ± 0.7*	6 ± ?*	7.2 ± 2.1	2.83 ± 0.95
K_{e3}	9.1 ± 4.1	7.9 ± 3.5	2 ± 2	2.6 + 2.2* - 1.7	5 ± 3.5*	3.9 ± 1.6	3.23 ± 1.30
Primary Beam	Cosmic rays	6.2-Bev protons (Bevatron)	6.2-Bev protons (Bevatron)	4.8-Bev protons (Bevatron)	2.9-Bev protons (Cosmotron)	6.2-Bev protons (Bevatron)	6.2-Bev protons (Bevatron)
Target	Emulsion stack	Emulsion stack	Ta	Ta	Cu	Cu	Cu
K production angle	0–180°	90° favored	90°	90°	60°	90°	90°
K energy (Mev)	Various	100–240	100	126	63	114	114
Proper time of flight (seconds)	$< 5 \times 10^{-10}$	$3-9 \times 10^{-10}$	1.5×10^{-8}	1.2×10^{-8}	2.16×10^{-8}	1.35×10^{-8}	1.35×10^{-8}

* Based on a fraction of the complete spectrum.

efficiencies derived by assuming 100% efficiency for τ's and a τ abundance of 5.6%. The numbers in columns 4, 5, and 6 are as quoted in the references except that we have computed the uncertainties on the Rochester results on the basis of the number of events of each type found. Statistics in the table are based upon the square root of the number of events and therefore have the significance of standard deviations only for those cases with large numbers of events.

In the last five rows of Table V are given the conditions of exposure of the nuclear emulsion stacks. With one possible exception there are no significant variations in the relative yield of K mesons of different types under the different exposure conditions. The one possible exception is the K_{e3}, which appears from Table V to be found less frequently under conditions of longer flight time. Specifically, the combined short time-of-flight data of GS and EP give 10 K_{e3} compared to 94 $K_{\pi 2}$ and $K_{\mu 2}$. The combined long time-of-flight results from MIT, Dublin, our work gives 13 K_{e3} compared to 326 $K_{\pi 2}$ and $K_{\mu 2}$. With these data and the equal lifetimes of 1.2×10^{-8} second for the $K_{\pi 2}$ and $K_{\mu 2}$ [13] we can determine the K_{e3} lifetime, assuming the abundances at production to be the same under all conditions of exposure. The result for the K_{e3} mean lifetime is 0.62×10^{-8} second, with a 90% probability of its lying between 0.47 and 0.94×10^{-8} second. Conversely, if we assume both that the relative production abundances under all conditions are equal and that the K_{e3}, $K_{\pi 2}$, and $K_{\mu 2}$ have the same lifetime, the purely statistical probability of obtaining such poor agreement between the short- and long-flight-time K_{e3} abundances is less than 0.02. Further study is required to resolve this discrepancy or to verify the difference in the K_{e3} behavior.

4. – Range Measurements on $K_{\mu 2}$ and $K_{\pi 2}$ Secondaries.

4.1 Method. – The measurement of the range of each particle consisted of adding the chords between points where the track made large single scatters or accumulated multiple scatters of at most 10°. This range includes the air gaps between pellicles and therefore, when multiplied by the gross density of the stacked emulsion, gives the range in g cm^{-2}.

(13) V. Fitch and R. Motley, Phys. Rev. 101, 496 (1956); Alvarez, Crawford, Good, and Stevenson, Phys. Rev. 101, 503 (1956).

The gross density was measured by the following procedure. The emulsion stack was first clamped tightly, with no tissue paper spacers, between 3/4-in. bakelite plates by means of bolts going through holes punched in the pellicles. All outside edges were machined smooth. The stack density was then determined by over-all weight and dimensions to be 3.80 ± 0.02 g cm^{-3}. The error is derived from the fluctuations in the thickness of the stack as measured at twelve different places.

The projected distances (Δx, Δy) between points were obtained by taking differences between the microscope stage screw readings. For each chord, Δz was taken equal to the number of plates traversed multiplied by the average apparent plate thickness before development obtained from the over-all thickness of the stack. Thus the air gaps are included in both the range and the density measurements. The individual plates were aligned by brass tabs which were glued on the corners with respect to x-ray fiducial marks.

The range-energy curve used[14] was calculated for an emulsion density of 3.815 g cm^{-3}, and the measured ranges must be transformed correspondingly. If the difference between this value and our measured density was due only to the air gaps in the stack the ranges in centimeters would transform inversely as the ratio of the densities. If part of the difference was due to the water content of the emulsions--an exact calculation would have allowed for the change in stopping power with water content--that is, if the pellicle density, assumed to be 3.815, was actually 3.825. For example, in this humidity region the density ratios must be corrected by addition of a quantity that is equal to 0.05 times the relative difference in density $(\frac{\Delta\rho}{\rho})$ [5].

In order to estimate the actual emulsion density, and hence the stopping power of our stack, we have measured the ranges of 46 nearly flat secondaries from $\pi - \mu$ decays, each contained within a single pellicle. These tracks were picked with a dip angle such that a 10% uncertainty in the shrinkage factor would lead to an error of less than 0.25% in the range of the muon. The average muon range obtained was 596.4 ± 6 microns, which agrees with that obtained by the G-Stack Collaboration[7] of 597.8 ± 2.1 microns for a density of 3.825 g cm^{-3}. Thus the uncertainty in stopping power due to the uncertainty of water content is less than 0.05%. This represents a negligible contribution to the errors in the $K_{\mu 2}$ and $K_{\pi 2}$ secondary ranges.

(14) W. H. Barkas and D. M. Young, Emulsion Tables. I. Heavy-Particle Functions, UCRL-2579 (Rev.), Sept. 1954.

4.2 Mass of the $K_{\mu 2}$ and $K_{\pi 2}$ from Ranges of the Secondaries. – The range distributions of the 20 muons and 23 pion secondaries that stopped in the stack are given in Fig. 4. Shown also are the standard deviations of the experimental distributions, which agree well with the theoretical range straggling. The mean ranges for the stack density of 3.80 g cm^{-3} are

$$R_{\mu} = (20.90 \pm 0.13) \text{ cm},$$
$$R_{\pi} = (11.70 \pm 0.065) \text{ cm}.$$

These ranges have been converted to a density of 3.815 g cm^{-3}, and the energies computed corresponding to these ranges, assuming the decay schemes

$$K_{\mu 2} \rightarrow \mu^{+} + \nu,$$
$$K_{\pi 2} \rightarrow \pi^{+} + \pi^{0},$$

and are shown in Table VI.

Table VI. – Ranges and energies of $K_{\mu 2}$ and $K_{\pi 2}$.

	Secondary range Density = 3.815 g cm^{-3}	Secondary energy
$K_{\mu 2}$	20.84 ± 0.13 cm	152.36 Mev
$K_{\pi 2}$	11.65 ± 0.067 cm	107.67 Mev

The K-particle masses are computed from these energies by use of the following pion and muon masses:[15],[16]

$$M_{\pi^+} = 273.3 \text{ m}_e,$$
$$M_{\pi^-} = 272.8 \text{ m}_e,$$
$$M_{\pi} - M_{\pi^0} = 8.8 \text{ m}_e,$$
$$M_{\mu^+} = 206.9 \text{ m}_e,$$

The results are:

$$M_{K_{\mu 2}} = (964.8 \pm 2.4) \text{ m}_e,$$
$$M_{K_{\pi 2}} = (964.2 \pm 1.8) \text{ m}_e,$$

(15) Barkas, Birnbaum, and Smith, Phys. Rev. 101, 778, (1956).
(16) W. Chinowsky and J. Steinberger, Phys. Rev. 93, 586 (1954).

where the errors given are due only to the standard deviation of the mean of the experimental range straggling.

Listed for comparison are the mass values from other laboratories, computed by use of the Barkas and Young range-energy curves.[14]

	$K_{\mu 2}$	$K_{\pi 2}$
G-Stack[7]	962.8 ± 4	969.3 ± 3
E.P.[8,19]	952 ± 4	969 ± 4
M.I.T.[9]	962.4 ± 5	963.6 ± 4.3

The curves from Baroni et al.[17] give consistent values for the $K_{\pi 2}$ mass but raise the $K_{\mu 2}$ mass about 13 m_e.

4.3 Discussion of Results. – Besides the quoted statistical errors the uncertainty in the value of the π mass contributes to an error of the order of ± 1 m_e in the K mass. The 1/2% uncertainty in the density becomes ± 1.2 m_e for the $K_{\pi 2}$ mass and ± 2 m_e for the $K_{\mu 2}$ mass.

As a check for further systematic errors, we remeasured all the pion secondaries, and found a negligible change in the mean range caused by the measurement procedure.

There is also the question as to the reliability of the range-energy relation. Recently Barkas et al.[18] have made an experimental determination of the ranges of pions of known energy for five values of energy up to about 100 Mev. They have recalculated the Barkas-Young values normalized to these experimental points. In the region above the last experimental point, the curve is extrapolated theoretically as before. With this new relation our mass values become

$$M_{K_{\mu 2}} = (965.8 \pm 2.4)\ m_e,$$

$$M_{K_{\pi 2}} = (962.8 \pm 1.8)\ m_e.$$

(17) Baroni, Castagholi, Cortini, Franzinetti, and Manfredini, CERN Report BS9.

(18) Barkas, Barrett, Cuer, Heckman, Smith, and Ticho, High-Velocity Particle Ranges in Emulsion, UCRL-3254, Jan. 1956. and W. H. Barkas, private communication.

For comparison, the mass of the τ[5] computed from the Q of the decays in this stack, and from one other stack treated in a similar manner, is

$$M_\tau = 966.1 \pm 0.7.$$

5. - Primary Mass.

The masses of the various types of K particles have also been measured by the primary range-momentum method. Measurements were made only on those tracks whose secondaries had been identified. Ranges of the K particles were measured along the track by the same method as were the secondaries. The momentum of each particle was determined from its entrance position in the stack, by measurement of the range of the protons entering the same position and hence their momentum. In the case of the protons, the measured ranges were actually projected ranges, and a correction to account for the range shortening due to multiple scattering effectively increased the K-meson mass by about 2 m_e. In addition, the different energy loss of K's and protons in the air path through the deflecting magnet and subsequent field-free region ahead of the stack required a mass correction of from 6 to 8 m_e on each particle, varying slightly with the incident momentum. Details of these and other corrections appear elsewhere[4].

The final corrected values of the masses, with the number of particles measured for each variety, are shown in Table VII.

Table VII. - Masses by Range-Momentum Method

Type	Mass (m_e)	No. Measured
τ	966.3 ± 2.1	77
τ'	967.7 ± 4	21
$K_{\mu 2}$	967.2 ± 2.2	96
$K_{\pi 2}$	966.7 ± 2.0	54
$K_{\mu 3}$	969 ± 5	12
K_{e3}	967 ± 8	6

6. - Conclusions.

We have measured the masses of the various decay modes of positive K mesons by two independent methods. The first is the measurement of the Q of the decay for the $K_{\mu 2}$, $K_{\pi 2}$, and τ; the second is the range-momentum method applied to the primaries. In the first method, the largest mass difference, that of $M_\tau - M_{K_{\pi 2}}$, is $(3.3 \pm 2.4)m_e$. The error includes (a) $\pm 1.9\ m_e$, statistical standard deviation; (b) $\pm 1.4\ m_e$, for possible variation in stack density; and (c) $\pm 0.6\ m_e$, for the uncertainty in pion masses. If the uncertainty of the range-energy relation is included the significance of the small mass difference decreases.

In the second method the masses are all the same within experimental error. In particular $M_\tau - M_{K_{\pi 2}}$, is $(-0.4 \pm 2.9)m_e$.

It is shown in Section III that our data on the relative abundances are the same as those taken under entirely different conditions of exposure and flight time, with the possible exception of the K_{e3}. If we also consider the equality of the masses it appears that we are observing different decay modes of the same particle.

However, this conclusion is in strong contradiction with the most likely spin and parity assignments of the τ meson (0^- or 2^-), which configurations are not possible for a $K_{\pi 2}$. Various theoretical and phenomenological descriptions have been proposed in order to resolve this dilemma, none of which are really satisfactory. For example, the cascade scheme[3] demands at least 10 m_e difference between the τ and $K_{\pi 2}$ to account for the observed half life for a $0 \rightarrow 0$ spin transition. This mass difference is well outside our experimental errors. Furthermore, neither the $K_{\pi 2}$[19] nor the τ is believed to have spin one, hence transitions $0 \rightarrow 1$ and $1 \rightarrow 0$ are not considered.

Transitions from $0 \rightarrow 2$ or $2 \rightarrow 0$ demand about 3 m_e to account for the observed half lives. The experiment of Alvarez et al.[20] shows that any γ-rays accompaning the transition $\tau \rightarrow K_{\pi 2}$ must be less than 1 m_e total energy, thus ruling out spin changes of ± 2. The possibility of the reverse transition, viz. $K_{\pi 2} \rightarrow \tau + \gamma$, is not excluded by the above experiment. In addition, a $2^+ \rightarrow 2^-$

---

(19) B. J. Moyer and J. Osher, private communication.

(20) Alvarez, Crawford, Good, and Stevenson, Proceedings of Sixth Annual Rochester Conference on High-Energy Physics, 1956.

transition requires only a 6 kev mass difference to give the observed half life, and no experiment to date has had sufficient sensitivity to detect a mass difference this small. However we believe that the zero spin assignments are the most probable and therefore the cascade scheme is unsatisfactory.

Other suggestions[21, 22, 23], while accounting for the mass degeneracy, must rely on an accident of nature to explain the half-life degeneracy. A more recent proposal, now being studied by Bludman and Ruderman[24], has been to postulate the existence of a scaler π^{o} in addition to the usual pseudoscaler π^{o}, with the result that the neutral and positive K particles have different parity. Then the positive τ and $K_{\pi 2}$ could both be 0^{-}.

The reader is referred to the proceedings of the 1956 Rochester Conference[25] for discussions of other theories that would have the τ and $K_{\pi 2}$ be the same particle.

---

(21) T. D. Lee and C. N. Yang, Phys. Rev. 102, 290 (1956); M. Gell-Mann, private communication.

(22) S. Bludman, Interpretation of K-Meson Decays, UCRL-3271, Jan. 1956.

(23) M. Lynn Stevenson, The Ratios of Lifetimes of Heavy Mesons and Hyperons as Predicted by Phase Space, UCRL-3275, Feb. 1956.

(24) S. Bludman and M. Ruderman, private communication.

(25) Proceedings of Sixth Annual Rochester Conference on High Energy Physics, 1956.

7. - Acknowledgments.

This experiment has been carried out with the guidance and encouragement of Professor Chaim Richman. It could not have been successfully completed without the help of many other people. Our thanks are due to Mr. C. Waller and the group at Ilford Ltd. for their cooperation in making the large emulsion stack used. Dr. Edward Lofgren and the members of the Bevatron staff aided in the successful exposure of the stack. Mr. Leroy Kerth aided in the design and setup of the strong-focusing spectrometer.

The emulsions were mounted on glass supplied with a grid coordinate system developed by Mr. Philip Carnahan. The processing of the stack was a group effort, with many late shifts taken by Mr. Jack Sandweiss.

Some of the secondaries were followed by Dr. Ludwig van Rossum and Dr. Stanley Leonard.

One of the most important phases of the work, that of scanning the stack, was done by Mrs. Beverly Baldridge, Miss Irene d'Arche, Mrs. Edith Goodwin, Mrs. Marilynn Harbert, and Miss Kathryn Palmer. Range measurements of primaries and τ and π-μ decays were done by Mr. Victor Cook, Mr. George Preston, and Mr. Norman Thomas. We are grateful for the patient and careful work of all of this group.

This work was done under the auspices of the U. S. Atomic Energy Commission.

Appendix.

Effect of Efficiency of Detection of K Secondaries on the Relative Abundances. – As mentioned in Section 2.2, the over-all efficiency for detection of K secondaries by the scanners is 85%. Since 8% of the K particles yield secondaries of ionization exceeding twice the minimum value, for which the efficiency is presumably 100%, this implies that 16% of the lightly ionizing secondaries escape detection. We shall consider how this loss affects the relative abundances of the predominant decay modes $K_{\pi 2}$ and $K_{\mu 2}$. (The statistical errors on the frequencies of the rare modes K_{e3} and $K_{\mu 3}$ are at present so large that small affects due to scanning inefficiency will not be considered).

A $K_{\pi 2}$ or $K_{\mu 2}$ secondary may escape detection for two main reasons. (a) Fluctuations in grain density occur, and a chance absence of grains close to the point of decay can lead to failure to pick up the track. (b) The stopping point of the primary particle may be close to the emulsion surface, so that if the secondary is directed outwards, its track may be missed because of its shortness, or the somewhat lower grain density near the top surface of the emulsion, or the presence of surface markings at the glass interface.

In (a), the probability of detection depends on the mean grain density, which is 15% greater in the tracks of $K_{\pi 2}$ secondaries than for $K_{\mu 2}$. The scanners scrutinize a roughly spherical volume, of ~50 μ radius about the end point of each stopping particle, for evidence of a secondary. Assuming a random distribution of grains along the secondary tracks, we have calculated the expected detection efficiency for each decay mode, on the simplifying assumption that some minimum number of grains must occur along the first 50μ of track in order for the secondary to be detected. For a given value of the true ratio $Ro = \frac{N_{K_{\mu 2}}}{N_{K_{\pi 2}}}$, we can then find the expected ratio R in terms of the total efficiency $\mathcal{E}$ for detecting both types of secondary. We find that $S = R/Ro$ varies almost linearly with $\mathcal{E}$, and that for the measured value of $\mathcal{E} = 84\%$, $S = 0.89$. Thus, for $R = 1.93 \pm 0.29$, the true ratio becomes $Ro = 2.12 \pm 0.30$. We feel that this value of Ro will be, if anything, an over-estimate, for the reasons given above: (a) it is certain that fluctuations of grain density over distances less than 50μ will (in many cases) be of importance in detecting the track; and since these fluctuations will be greater than those over 50μ lengths, the bias in favor of $K_{\pi 2}$ secondaries will be correspondingly less. (b) surface effects may account for a 5% to 10% loss.

Figure Captions

1. Diagram of strong-focusing spectrometer.
2. Distribution of normalized blob density for flat secondaries. Normalization is to π tracks of 210 Mev in the emulsion stack and to identified $K_{\mu 2}$ secondaries.
3. Distribution of normalized blob density for identified $K_{\mu 2}$ secondaries.
4. Distribution of $K_{\mu 2}$ and $K_{\pi 2}$ secondary ranges. The dashed line shows the position of the mean of the distribution. σ_{exp} is the experimental standard deviation and σ_{th} is the theoretical straggling.

STRONG - FOCUSING SPECTROMETER

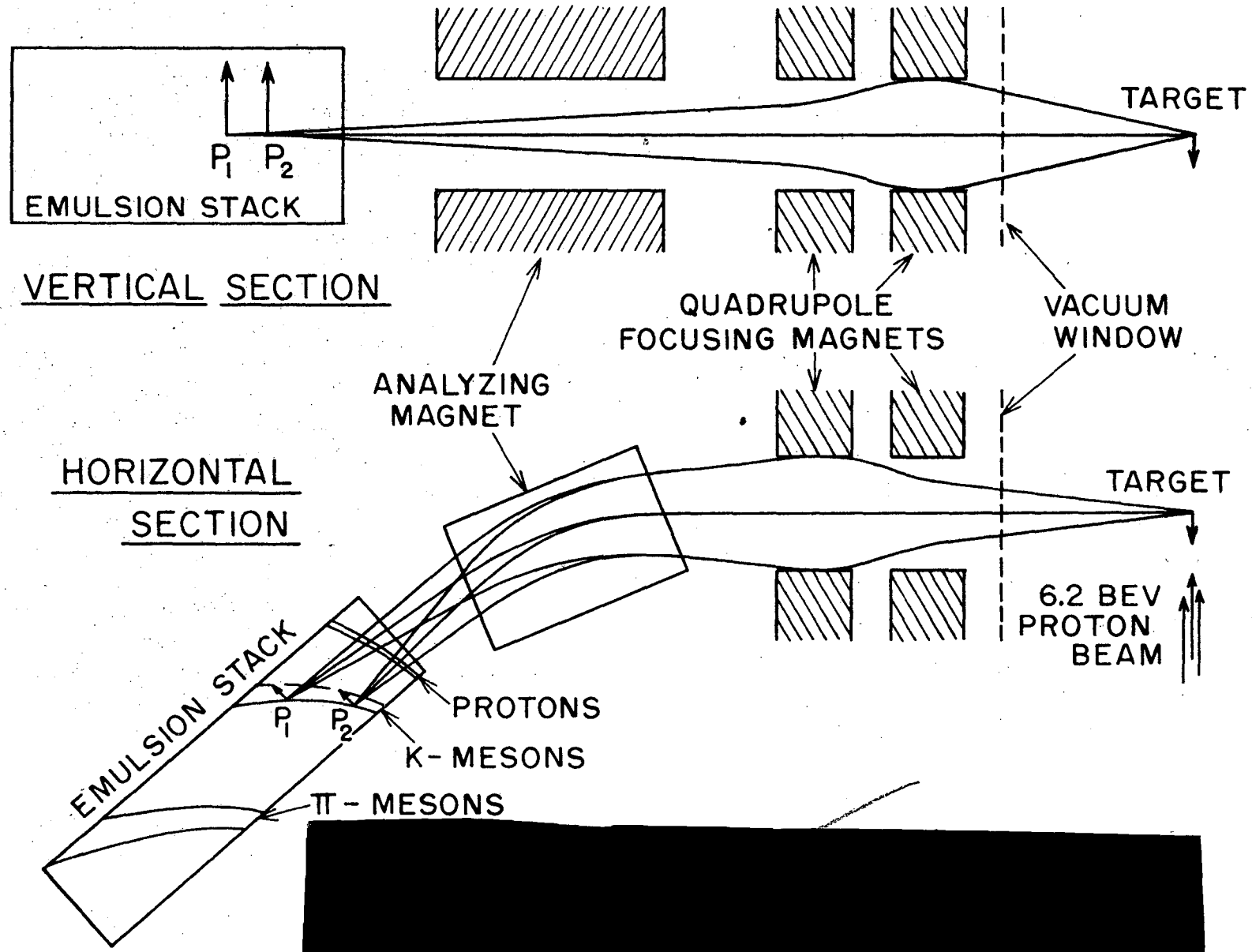

[redacted]

MU-10604

24256-1

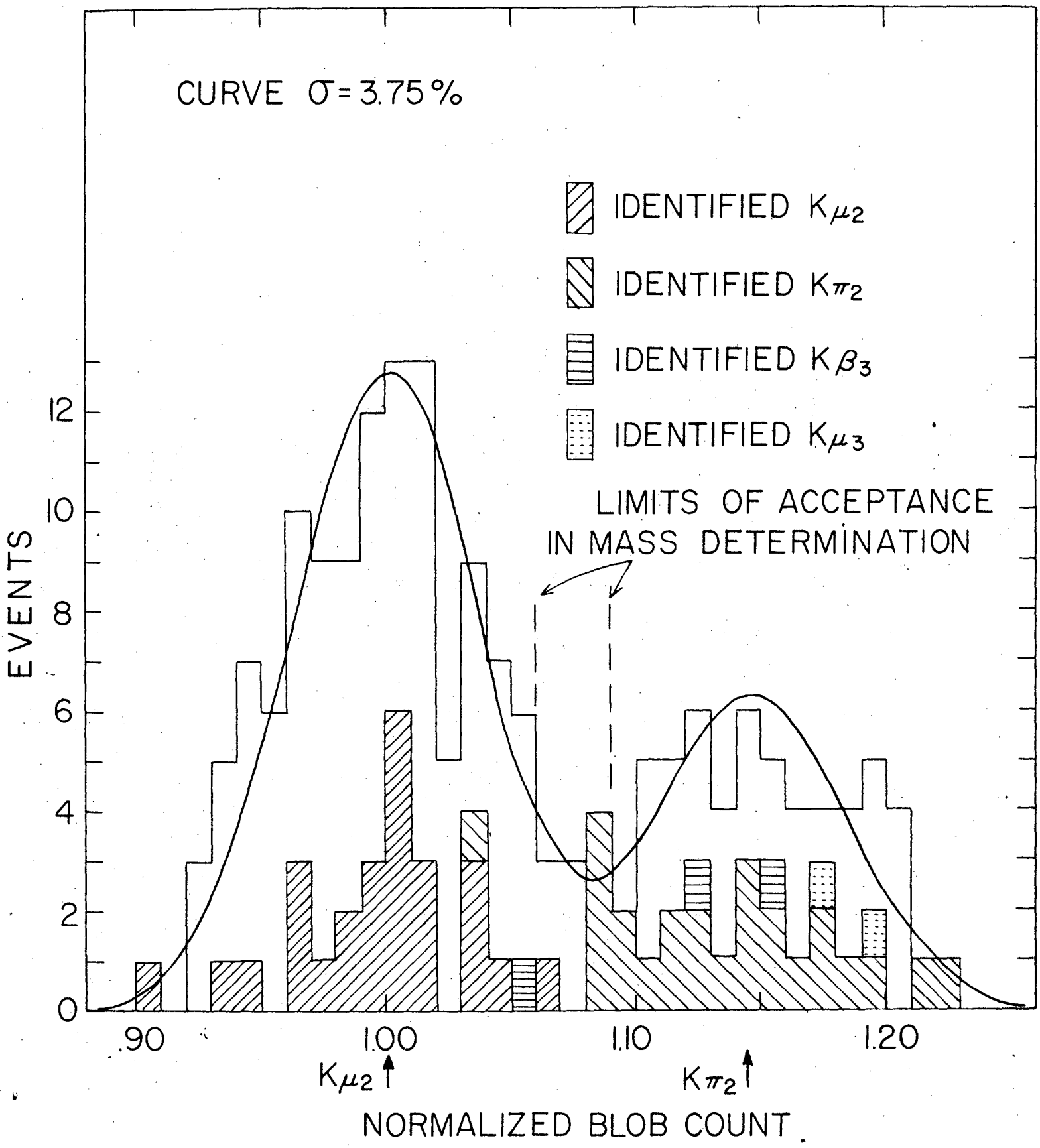
CURVE σ = 3.75%
IDENTIFIED Kμ2
IDENTIFIED Kπ2
IDENTIFIED Kβ3
IDENTIFIED Kμ3
LIMITS OF ACCEPTANCE IN MASS DETERMINATION
EVENTS
0
2
4
6
8
10
12
.90
1.00
1.10
1.20
Kμ2
Kπ2
NORMALIZED BLOB COUNT

242 54-1

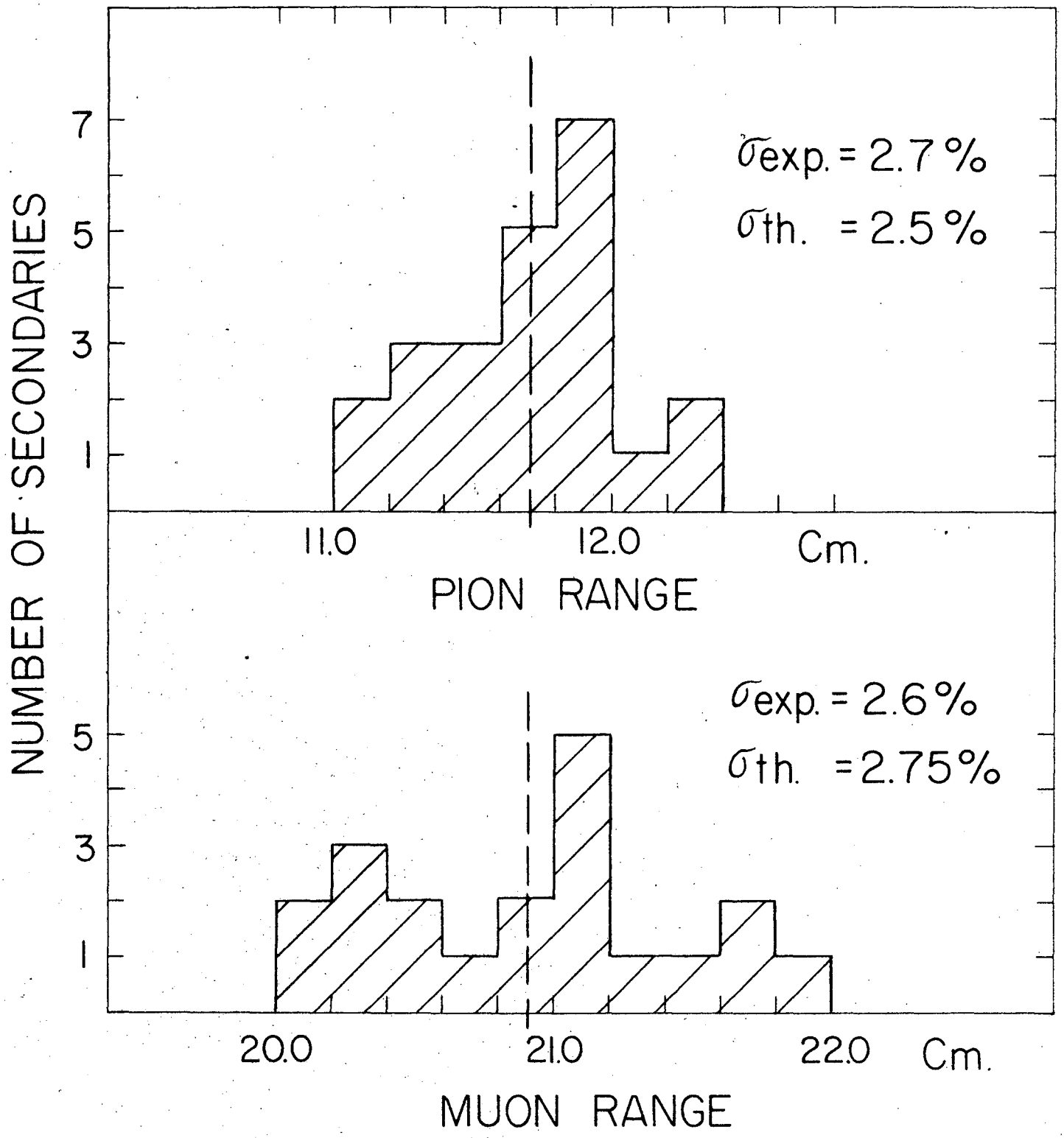
NUMBER OF SECONDARIES
7
5
3
1
σexp. = 2.7 %
σth. = 2.5 %
11.0
12.0
Cm.
PION RANGE
5
3
1
σexp. = 2.6 %
σth. = 2.75 %
20.0
21.0
22.0
Cm.
MUON RANGE

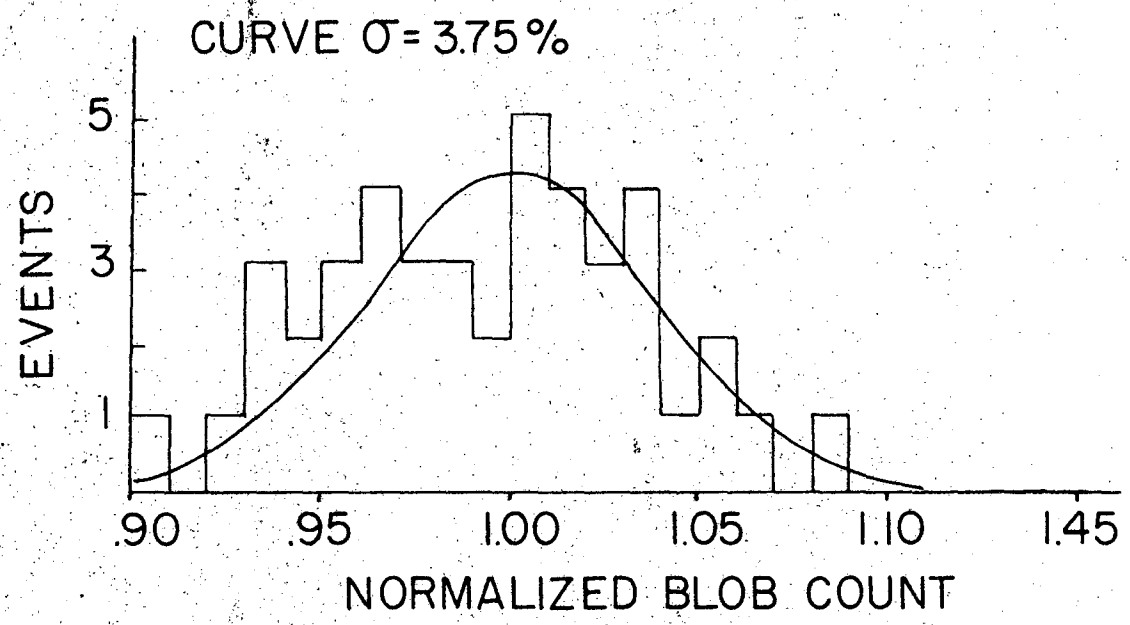
CURVE σ = 3.75%
EVENTS
5
3
1
.90
.95
1.00
1.05
1.10
1.45
NORMALIZED BLOB COUNT

245371